Polarization properties of light emitted by a bent optical fiber probe and polarization contrast in scanning near-field optical microscopy

Yasuyuki Mitsuoka,[a] Kunio Nakajima, Katsunori Homma, Norio Chiba, Hiroshi Muramatsu, and Tatsuaki Ataka
Technology Center, Seiko Instruments Inc., 563 Takatsuka-shinden, Matsudo, Chiba 270-2222, Japan

Katsuaki Sato
Faculty of Technology, Tokyo University of Agriculture and Technology, 2-24-16 Nakacho, Koganei, Tokyo 184-8588, Japan

(Received 1 August 1997; accepted for publication 18 January 1998)

This article describes the polarization properties of light emitted by a bent optical fiber probe which is used for scanning near-field optical microscopy operated in atomic force mode (SNOM/AFM). SNOM/AFM can be applied to the observation of magnetic domains by imaging polarization contrast in transmission mode. A bent optical fiber probe with a subwavelength aperture is vibrated vertically as a cantilever for atomic force microscopy. Plane polarized light with an extinction ratio of better than 70:1 was emitted by the aperture by controlling the polarization state of incident light to the probe. A particular transverse polarization component of light transmitting a sample is selected by a polarization analyzer and detected. We obtained clear polarization contrast images of 0.7 μm length bits written with a conventional method using a focused laser beam on a bismuth-substituted dysprosium-iron-garnet film. © *1998 American Institute of Physics.*
[S0021-8979(98)07408-8]

I. INTRODUCTION

Scanning near-field optical microscopy (SNOM),[1–5] which can obtain a resolution beyond the diffraction limit by placing a subwavelength source or detector in close proximity to a sample, has contributed greatly to the investigation of optical properties at the nanometric level. In many studies, SNOM has provided the transmittance (or the reflectance) distribution and the spectral characteristics of the sample by measuring two components of light; amplitude and frequency (wavelength). The other component, phase, is rarely measured by SNOM. Although the detection of the phase change of polarized light can improve the sensitivity of SNOM and provide other useful information, the polarization state of light in the near-field region is a complicated issue and has not yet been discussed sufficiently.

Control of the polarization state of light emerging from the aperture and analysis of the polarization state of light coming from the sample can expand the applications of SNOM. For example, the fields of magneto-optics, liquid crystal, and photoluminescence are scientifically and technologically interesting for SNOM with polarized light. In magneto-optics, microscopy with higher resolution and sensitivity has been required to observe the smaller magnetic domains and walls of ferromagnetic materials because bit sizes in erasable data storage devices, such as magneto-optical disks and magnetic disks, are shrinking according to the need to increase storage capacity.

Many methods to observe the magnetic domains have been proposed such as polarizing microscopy, Lorentz transmission electron microscopy,[6] magnetic force microscopy (MFM),[7] and spin polarized scanning electron microscopy.[8] However, each of them has drawbacks in areas such as resolution, sensitivity, sample preparation, instrument costs, and quantitative results. For example, MFM has a good resolution but it is difficult to quantify the magnetic properties of a sample from the MFM signal.

SNOM with polarized light has a high resolution and the possibility to overcome the disadvantages through the introduction of quantitative and sensitive measurement techniques used in magneto-optics. Most efforts of SNOM have used the lateral shear force feedback in which a straight optical fiber probe with a small aperture vibrates laterally on the sample surface to control the distance between the tip of the probe and the sample. By using this feedback technique, SNOM can be used to observe the magnetic domains in transmission utilizing the magneto-optical effect.[5,9–11] In other studies, Silva *et al.* have demonstrated the near-field imaging of magnetic domains in reflection with a silver particle optically excited at the surface plasmon resonance frequency as a near-field probe, and with a Newton ring interferometer for the separation of the probe and sample.[12,13]

We have already developed scanning near-field optical microscopy operated in atomic force mode (SNOM/AFM),[14–16] in which a bent optical fiber probe with a small aperture vibrates vertically on the sample surface to control the tip-sample separation. This dynamic feedback technique, which is originally used in an atomic force microscopy (AFM), has several advantages such as easy operation with soft samples because the interaction between the probe and the sample can be controlled, and good performance for samples in liquid because the round optical fiber cantilever can reduce the viscous resistance of liquid. We also expect that a probe controlled by AFM feedback can

[a]Corresponding author; electronic mail: mitsuoka@tk.sii.co.jp

 © 1998 American Institute of Physics

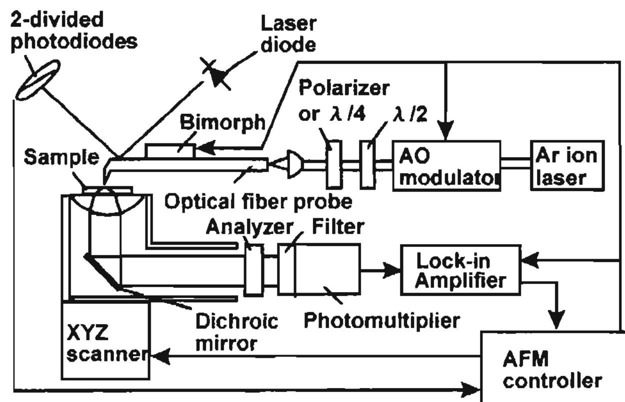

FIG. 1. Schematic diagram of a SNOM/AFM system for near-field imaging of polarization contrast in transmission mode.

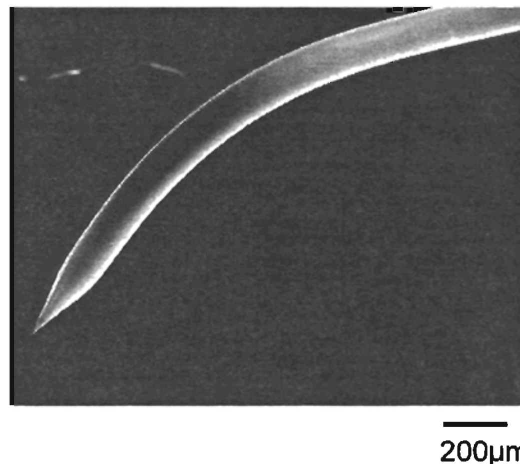

FIG. 2. Scanning electron micrograph of an optical fiber probe used in the SNOM/AFM system.

trace the rough surface of the sample more accurately and at less risk of damaging the probe and the sample than one controlled by shear force feedback.

In this article, we describe the polarization properties of the light emitted by the aperture of a bent optical fiber probe, and demonstrate the polarization contrast imaging of magnetic domains with the Faraday effect by SNOM/AFM.

II. EXPERIMENTAL SETUP

Figure 1 shows a schematic diagram of the SNOM/AFM system for near-field imaging of polarization contrast in transmission mode. An optical fiber probe mounted on a bimorph is vibrated vertically against the sample stage at the resonance frequency (typically 10–40 kHz). A 680 nm laser beam reflected on a polished surface of the probe is detected by a two-divided photodiode and the change of the vibration amplitude of the probe is monitored. The vibration amplitude decreases as the tip of the probe approaches the sample surface, thus controlling the tip-sample separation by maintaining the amplitude at a constant value in typical imaging. The vibration amplitude is from 70 to 98% of the free vibration amplitude, which is varied at 10–100 nm by the voltage applied to the bimorph. This amplitude control method makes it possible to change the interaction force between the probe and the sample.

Figure 2 shows the scanning electron micrograph of the optical fiber probe. A single-mode optical fiber with a sharpened tip is bent to control the distance between the tip of the probe and the sample surface, allowing it to be used as an AFM cantilever in dynamic mode. The single-mode optical fiber whose core and cladding is 3.2 and 125 μm in diameter respectively is pulled to form the tip, and bent at 0.5 mm from the apex of the tip by the irradiation of a CO_2 laser. The bent angle is about 80°. An aperture at the apex of the probe is formed by coating the side of the tapered probe with 100–150 nm thick aluminum film.

A 488 nm air-cooled argon ion laser with an output power of 20–80 mW is used as the light source. The beam of the argon ion laser is modulated by an acousto-optic (AO) modulator at the probe vibration frequency to improve the signal-to-noise ratio of the optical signal, and coupled to the other end of the probe. By adjusting the phase of the AO modulation, light is emitted by the aperture only in the range of the least tip-sample separation in the probe vibration cycle to improve the resolution of the optical image. The duty ratio of the emission (the emitting time/the vibration period) is typically 20–30%. Half- and quarter-wave plates or a polarizer are placed before the input fiber coupler. The desired polarization state of the incident beam to the probe is produced by changing the orientation of the wave plates. Because the optical fiber probe has retardation and perturbation properties, the polarization properties of the light emitted by the aperture of the probe can be controlled by changing the polarization state of the incident beam. After transmitting the sample, the light emitted by the probe is detected by an uncooled photomultiplier through a collimation lens, a dichroic mirror, an analyzer and an optical filter. The dichroic mirror is used instead of an aluminum mirror to reduce the difference of the reflectance between the p- and s-polarized lights. A particular transverse polarization component selected by the analyzer is measured in the far field. The detected signal is amplified by a lock-in amplifier to reduce the noise in the signal.

III. RESULTS AND DISCUSSION

A. Basic performance of SNOM/AFM

Topographic and near-field optical images of a test sample of chromium film with a size of 2×2 μm^2 and thickness of 20 nm on a quartz substrate are shown in Figs. 3(a) and 3(b). The scanned area was 5×5 μm^2. The vibration amplitude of the probe was about 10 nm. The elevated parts in the topographic image were the chromium patterns, which correspond to the dark areas in the near-field optical image because of the lower transmittance of the chromium film. Figure 3(c) shows an optical intensity profile which corresponds to line AA' in Fig. 3(b). The optical intensity in the profile is normalized by the average intensity on the quartz substrate. The width of the slope between the dark and bright part is about 70 nm on the 20–80% threshold. Because of the artifacts occurring in the near-field imaging, it is difficult to estimate the optical resolution and the aperture size by scan-

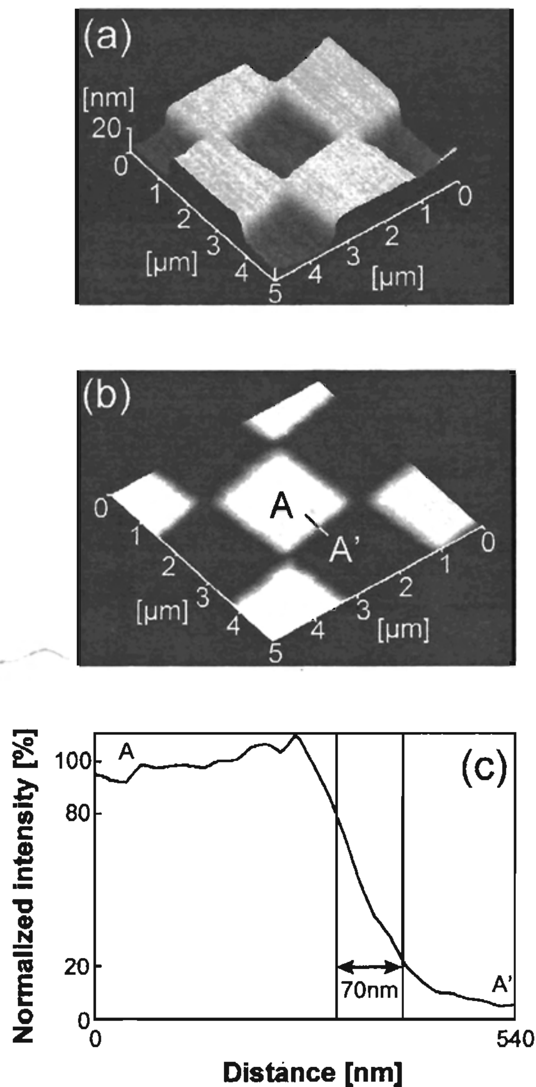

FIG. 3. (a) Topographic image, (b) optical image of 20-nm-thick chromium patterns on the quartz substrate, and (c) optical profile corresponding to the line in (b), which are all observed by SNOM/AFM. The lock-in time constant was 1 ms. The scan rate was typically between 0.25 and 0.5 lines/s. The bandwidth of the feedback loop to control the tip-sample separation is limited primarily by the mechanical resonance of the piezoelectric XYZ scanner. The scanner has a range of 50 μm and a resonance frequency of hundreds Hz. The vertical noise level to the sample surface in the topographic image was less than 0.5 nm.

ning across the topographical edge. However, the thickness of the chromium film is much smaller than the slope width, and the enhancement of the optical intensity at the edge is small. The aperture of this probe is roughly estimated to be 70 nm in diameter. The contrast of the near-field optical image is given by

$$\text{Contrast}=(I_q-I_{cr})/(I_q+I_{cr}), \tag{1}$$

where I_q and I_{cr} are the average signal intensity on the quartz substrate and on the chromium film, respectively. The external transmittance of the quartz substrate and that of the chromium film on the quartz substrate, measured by a conventional spectrophotometer was about 92% and 6.3% at a wavelength of 488 nm, respectively. In Fig. 3(c), the contrast is about 0.87, which is equivalent to that estimated from the external transmittance. Some emission sources other than the aperture, such as defects in the coated aluminum film on the probe, decrease the contrast of the near-field image much more than they decrease the resolution.

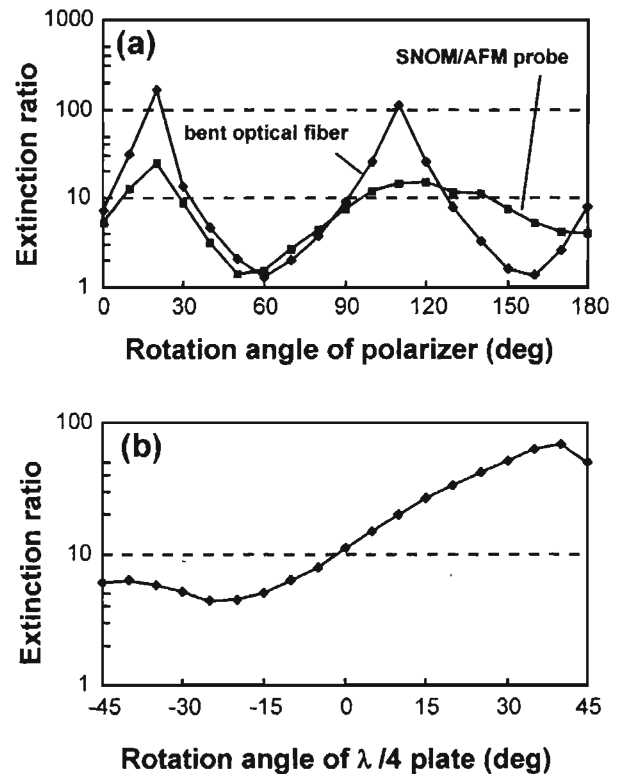

FIG. 4. (a) Extinction ratio of light emerging from the core of the bent optical fiber and the aperture of the SNOM/AFM probe vs the rotation angle of the polarizer, and (b) extinction ratio of light emitted by the aperture of the SNOM/AFM probe vs the rotation angle of the quarter-wave ($\lambda/4$) plate.

B. Polarization properties of the bent optical fiber probe

The polarization properties of the light emitted by the aperture were measured without a sample. This makes it possible to obtain the polarization effects of the aperture alone without the interaction between the aperture and the sample. The relation between the rotation angle of the polarizer placed before the fiber coupler and the polarization extinction ratio of the light emitted by the bent optical probe is shown in Fig. 4(a). The extinction ratio is the ratio of the maximum to the minimum intensity signal with respect to the orientation of the analyzer. In this study, the aperture of the probe and the contrast of the near-field optical image were estimated to be about 150 nm in diameter and 0.87 from the optical intensity profile of the chromium patterns, respectively. The light emitted by this probe with a relatively large aperture had enough intensity to be detected in the far field. Light emitted by the hollow defects on the coated aluminum film seemed to be negligible because of the good contrast of the near-field optical image.

The polarization property of the light emerging from the core of the bent optical fiber with a cleaved end is also plotted in Fig. 4(a). The bent angle of the fiber was the same as that of the probe. When plane polarized light was coupled at the input end of the fiber, the light emerging from the core of

the bent optical fiber was normally elliptically polarized, because the anisotropy in either stress or deformation of the core in the bend produces retardation. The polarization property of the bent fiber was shown to be the same as a quarter-wave plate with an optic axis, whose direction is considered to correspond to the bent direction. The bend of the fiber perturbed the polarization and provided a slightly low extinction ratio (100–200:1) compared with the high extinction ratio (>500:1) of an optical fiber without a bend.

The polarization property of the light emitted by the bent optical probe with a tapered end was similar to that of the bent fiber with a cleaved end, and showed a slight perturbation and anisotropy of the polarization. When the retardation of the incident light to the probe was adjusted adequately by a quarter-wave plate, plane polarized light with a polarization extinction ratio of better than 70:1 emerged from the aperture [Fig. 4(b)]. The plane polarization direction of the incident light to the probe was set by a half-wave plate at a polarizer angle of 140° in Fig. 4(a). The quarter-wave plate placed after the half-wave plate varied the retardation of the incident light. These results showed that the aperture or the tapered tip of the probe degraded the extinction ratio more strongly than bending the fiber did. Improvement of the fabrication process of the aperture, such as a perfectly circular aperture and smooth aluminum film, is required to increase the extinction ratio. By using an optical fiber with either a small photoelastic constant or a small diameter, the retardation caused by the stress in the bend should decrease.

C. Polarization contrast of magneto-optical film

We confirmed that SNOM/AFM is applicable to the observation of small magnetic domains in magneto-optical film in transmission mode using the Faraday effect. The sample was a 100-nm-thick bismuth-substituted dysprosium-iron-garnet film on a glass substrate. The film had a perpendicular magnetization of less than 30 emu/cm^3. The Faraday rotation angle of the sample was about 1.7° at the 488 nm wavelength by means of the far-field measurement. In the garnet film, bits with a size of about 3×1 μm and 0.7×1 μm were written by a conventional magneto-optical recording system using a focused laser beam. The bit length was varied by the irradiation pulse width of the writing laser beam.

A plane polarized light with high extinction ratio was emitted by the aperture by adjusting the polarization state of the incident light to the probe. Figure 5(a) shows a topographic image, and Figs. 5(b)–5(d) show the polarization contrast images corresponding to the topographic image when the analyzer was oriented to three different angles. The scanned area was 10×10 μm^2. The polarization contrast images have a good contrast and distinguish the recorded bits clearly. By changing the orientation of the analyzer the polarization contrast is lost [Fig. 5(c)] and inverted [Figs. 5(b) and 5(d)]. The Faraday effect caused the polarization direction of the light emitted by the aperture to be rotated upon passage through the garnet film. The opposite of the rotary direction (clockwise or counterclockwise) which depends on the magnetization (up or down) of the garnet film produces the polarization contrast by detecting a particular polarization component in the transmitted light of the garnet film. The topographic resolution depends on the apex shape of the optical fiber probe. The tip of the sharpened optical fiber was coated with 100–150 nm aluminum film. The aperture of the probe was estimated to be about 150 nm in diameter. The diameter at the apex of the probe was approximately 400 nm. The topographic image has lower spatial frequencies than the polarization contrast images. Figure 6(a) shows the polarization contrast image of small bits with a length of 0.7 μm in the garnet film. The optical intensity profile which corresponds to the line in Fig. 6(a) is shown in Fig. 6(b). The scanned area was 5×5 μm^2. The contrast of the polarization image is about 0.3. The resolution of the polarization contrast images is estimated to be beyond the diffraction limit of a conventional optical polarizing microscope, because small structures in the bits can be observed.

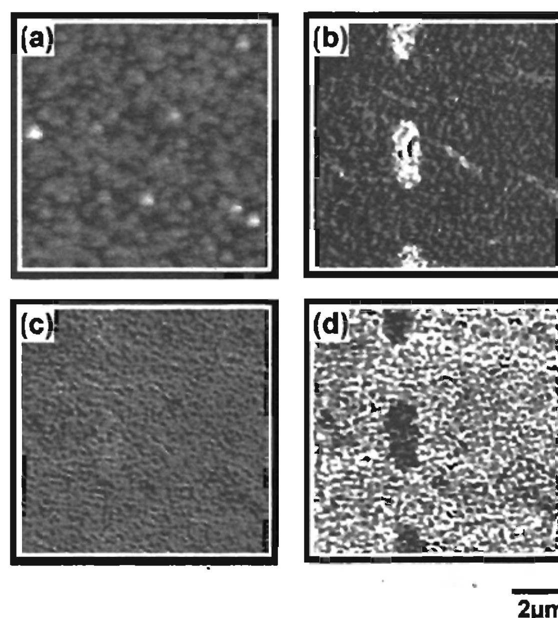

FIG. 5. (a) Topographic image and (b)–(d) polarization contrast images of magnetic domains in the garnet film at three different polarization states, which are all observed by SNOM/AFM.

Figure 7 shows (a) the topographic and (b) the corresponding MFM images of the garnet film. The scanned area was 15×15 μm^2. In the MFM tip fabrication, a thin magnetic film was coated on a sharp AFM tip. The diameter at the apex of the MFM tip was several tens nm. The topographic resolution in Fig. 7(a) is better than that of the SNOM/AFM. Compared to the polarization contrast image obtained by SNOM/AFM, the MFM image of the written bits has good resolution but a very low contrast of about 1×10^{-3}. The magnetization of this garnet film was much less than that of a magneto-optical disk media (typically 100–400 emu/cm^3). Magnetic force microscopy has difficulty in observing domains with small magnetization due to mapping of the gradients of the stray fields emanating from the surface. The SNOM/AFM system for the near-field imaging of polarization contrast seems useful with respect to a direct observation of magnetic domains using the magneto-optical effect.

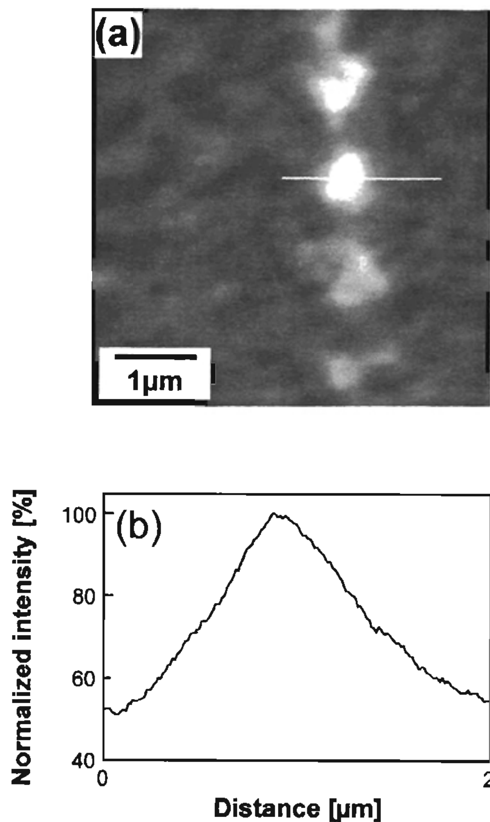

FIG. 6. (a) Polarization contrast image of magnetic domains with 0.7 μm length in the garnet film, and (b) optical profile corresponding to the line in (a), which are observed by SNOM /AFM.

D. Future demands of SNOM/AFM for polarization contrast

SNOM/AFM will create several improvements in the imaging of polarization contrast in the future. First, the resolution of the near-field optical image will be higher. The achievement of higher resolution requires a probe with a smaller aperture. However, decreasing the aperture size usually makes observing with lower noise level more difficult because of the weaker light emitted by the aperture. We are currently redesigning the structure of the tapered tip such as the tapered angle and the radius of the apex to obtain a smaller aperture while still emitting light with enough intensity. Second, the SNOM/AFM system is able to detect the change of the polarization state caused by the Faraday effect. However, in the case of detecting the smaller angle of the Kerr rotation to observe the magnetic domains in reflection mode, SNOM/AFM needs a higher sensitivity for the emission of plane-polarized light with a higher extinction ratio. The fabrication process of the probe will be improved to produce the perfectly circular aperture, smoothly coated aluminum film, and less stress in the bend. The polarization state of the incident light to the probe can also be adjusted more adequately. Third, the demonstration to observe the magnetic domains using SNOM/AFM showed only the qualitative results. The low sensitivity and insufficient accuracy of the conventional crossed-polarizer method makes quantitative measurement difficult. Utilizing the polarizing modulation technique with a photoelastic modulator would make a quantitative observation possible.

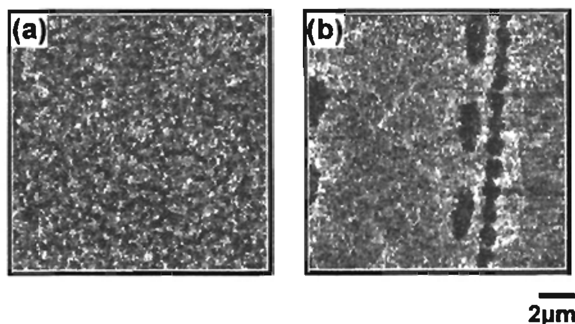

FIG. 7. (a) Topographic image and (b) MFM image of magnetic domains in the garnet film, which are observed by MFM.

Although experimental results help the investigations of the complicated imaging mechanisms, many issues of near-field polarization remain unresolved. For example, the near-field polarization properties considering the interaction between the aperture and the sample remain to be investigated. In this article, only the far-field polarization state of the light emitted by the aperture was measured. However, the SNOM/AFM system shows the advantageous potential to obtain the phase information and would become a useful tool for scientific researches at the nanometric level.

IV. CONCLUSION

We described the polarization properties of light emitted by the aperture of a bent probe used for a SNOM/AFM system. The bent probe operated as an AFM cantilever and showed retardation properties similar to a quarter-wave plate. Control of the polarization state of incident light to the probe by wave plates allows the light emitted by the aperture to have a polarization extinction ratio of better than 70:1. The applicability of SNOM/AFM to image polarization contrast was also demonstrated. By detecting a selected polarization component in the transmitted light of the garnet film, perpendicularly magnetized domains could be observed clearly as the polarization contrast caused by the Faraday effect.

ACKNOWLEDGMENTS

This work is supported in part by a grant-in-aid from the Ministry of Education, Science and Culture. The authors wish to thank Dr. N. Kawamura (NHK science and Technical Res. Lab.) for supplying the garnet film.

[1] A. Lewis, M. Isaacson, A. Harootunian, and A. Muray, Ultramicroscopy **13**, 227 (1984).
[2] D. W. Pohl, W. Denk, and M. Lanz, Appl. Phys. Lett. **44**, 651 (1984).
[3] E. Betzig, A. Harootunian, A. Lewis, and M. Isaacson, Appl. Opt. **25**, 1890 (1986).
[4] E. Betzig, J. K. Trautman, T. D. Harris, J. S. Weiner, and R. L. Kostelak, Science **251**, 1468 (1991).
[5] E. Betzig and J. K. Trautman, Science **257**, 189 (1992).
[6] J. N. Chapman, A. B. Johnston, and L. J. Heyderman, J. Appl. Phys. **76**, 5349 (1994).
[7] D. Rugar, H. J. Mamin, P. Guethner, S. E. Lambert, J. E. Stern, I. McFadyen, and T. Yogi, J. Appl. Phys. **68**, 1169 (1990).
[8] K. Koike and K. Hayakawa, Jpn. J. Appl. Phys., Part 2 **23**, L187 (1984).

[9] J. K. Trautman, E. Betzig, J. S. Weiner, D. J. DiGiovanni, T. D. Harris, F. Hellman, and E. M. Gyorgy, J. Appl. Phys. **71**, 4659 (1992).
[10] E. Betzig, J. K. Trautman, J. S. Weiner, T. D. Harris, and R. Wolfe, Appl. Opt. **31**, 4563 (1992).
[11] E. Betzig, J. K. Trautman, R. Wolfe, E. M. Gyorgy, P. L. Finn, M. H. Kryder, and C.-H. Chang, Appl. Phys. Lett. **61**, 142 (1992).
[12] T. J. Silva, S. Schultz, and D. Weller, Appl. Phys. Lett. **65**, 658 (1994).
[13] T. J. Silva and S. Schultz, Rev. Sci. Instrum. **67**, 715 (1996).
[14] M. Fujihira, H. Monobe, H. Muramatsu, and T. Ataka, Chem. Lett. **3**, 657 (1994).
[15] N. Chiba, H. Muramatsu, T. Ataka, and M. Fujihira, Jpn. J. Appl. Phys. **34**, 321 (1995).
[16] H. Muramatsu, N. Chiba, K. Homma, K. Nakajima, T. Ataka, S. Ohta, A. Kusumi, and M. Fujihira, Appl. Phys. Lett. **66**, 3245 (1995).